Climbing the anisotropy barrier of single-molecule magnets with spin-vibron interaction

V. Moldoveanu and R. Dragomir
National Institute of Materials Physics, Atomistilor 405A, Magurele 077125, Romania

(Received 3 March 2023; revised 30 June 2023; accepted 10 July 2023; published 20 July 2023)

Using the master equation approach, we look for fingerprints of the interaction between the localized spin S of a nanomagnet coupled to spin-polarized leads and its quantized vibrational modes. We find that the stationary and transient currents are sensitive to vibron-assisted transitions of the molecular spin on both sides of the anisotropy barrier. Such transitions are associated with vibron-dressed states and triggered under resonant conditions. Transport calculations are presented for two antiparallel configurations of the spin-polarized electrodes. In the first configuration, and far from a resonance point, a blockade is imposed on both the electronic and molecular spins via their exchange interaction. When sweeping the magnetic field through resonance, the spin-vibron interaction removes this blockade and allows the indirect reading of resonant transitions as the molecular spin climbs the left side of the anisotropy barrier. In the second configuration, the anisotropy barrier is overcome but the vibron-assisted transitions on the right side of the anisotropy barrier "delocalize" the molecular spin and do not allow the complete current-induced magnetic switching $-S \rightarrow S$. In both configurations, the stationary current increases on resonance, due to additional transport channels triggered by the spin-vibron coupling. Therefore, the switching of the spin-vibron coupling could be detected in future transport experiments.

DOI: 10.1103/PhysRevB.108.024416

I. INTRODUCTION

The magnetic and transport properties of single-molecule magnets (SMMs) have been investigated and measured for a long time and are by now well understood [1,2]. Fe_4 SMMs, manganese clusters, and lanthanide-based nanomagnets behave like giant molecular spins interacting with magnetic fields, itinerant electrons, or vibrational modes. Therefore, they serve as a workbench for investigations on the dynamics of localized magnetic moments.

A common feature of molecular nanomagnets is the so called anisotropy energy barrier of height DS^2, where D is the axial magnetic anisotropy coefficient. At very low temperatures, this barrier prevents transitions to excited states with spin quantum numbers $|S_z| < S$ [3]. Additionally, transverse anisotropy terms allow underbarrier transitions between the states of the lowest energy doublet $S_z = \pm S$, through quantum tunneling of magnetization (QTM). This switching mechanism is extensively studied in view of applications to spintronics and manipulation of molecular spin qubits (see the recent review [4] and references therein).

Operating the $2S + 1$ spin states as molecular qubits in scalable architectures remains a timely endeavor [5,6]. For example, Godfrin *et al.* [7] reported the successful implementation of the Grover algorithm using the nuclear spin states of a $TbPc_2$ molecular magnet. In the case of single-ion magnets (e.g., Gd^{3+}), coherent transitions between the $2S + 1$ states were measured and could be used to implement multiple-qubit protocols [8]. A theoretical study showed that the spin states of this $S = 7/2$ nanomagnet can be manipulated as molecular qudits [9].

To probe their excited states and magnetic anisotropy effects [10,11], the single-molecule magnets are attached to source and drain electrodes such that electrons tunnel sequentially on the lowest unoccupied molecular orbital (LUMO). Then the system is pushed to a charged configuration (i.e., a state containing one extra electron). Now, in typical transport measurements on SMMs, various interactions are activated and coexist: (i) the exchange interaction between the localized magnetic moment and the electronic spin (see the sketch in Fig. 1); (ii) the coupling between the charge and the vibrational modes of the system leading to a Franck-Condon blockade [12,13]; and (iii) the spin-mechanical coupling associated with intrinsic or external quantized vibrational modes (i.e., vibrons).

Up to now, the effects of the spin-vibron interaction were only identified in hybrid SMM-nanoresonator systems, where the nanomagnet is rigidly attached to a vibrating conductor (e.g., a conducting carbon nanotube supporting longitudinal stretching modes) [14,15].

On the theoretical side, one finds that the interactions mentioned above are investigated rather separately. For example, density-functional theory (DFT) calculations describe either the electric control of a Fe_4 molecule [16,17], the effects of the charge-vibron interaction [18], or the many-body transport properties [19]. Vibronic effects on the quantum tunneling of magnetization have been analyzed in a recent work [20].

Similarly, the role of the exchange interaction in the transport process has been mostly discussed in the absence of vibrational modes. An important result is that if the exchange coupling is not purely axial [see the discussion of Eq. (2) below], the charged states acquire a mixed spin structure that triggers a sequence of transitions to excited spin states [21] and even leads to the so called current-induced magnetic switching (CIMS) when at least one electrode is spin-polarized [22–24]. The main features of the CIMS are also presented in the review [25].

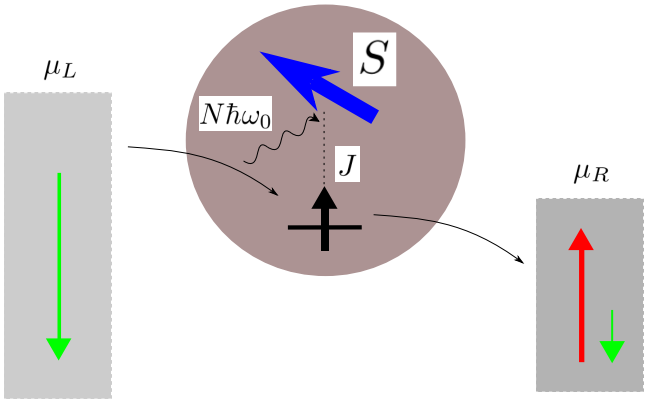

FIG. 1. A schematic picture of the SMM connected to spin-polarized electrodes with chemical potentials $\mu_{L,R}$. The quasi-antiparallel configuration corresponds to a fully spin-down polarized left electrode and a mostly spin-up polarized right electrode. The localized spin S and the electronic spin tunneling on the molecular orbital are coupled by the exchange interaction of strength J. Also, the N vibrons of frequency ω_0 generated along the tunneling processes by the charge-vibron interaction are coupled to the molecular spin.

Recently, it was shown that the effect of the exchange interaction on the spin-dependent conductance allows the electric reading of the electronic spin [26]. On the other hand, spin-vibron coupling effects on the transport properties have been discussed in connection to Kondo effects [27], vibrational cooling by a spin-polarized current [28,29], and vibron-induced renormalization of the anisotropy parameters [30]. To the best of our knowledge, the mechanically assisted magnetic switching in a SMM that is *directly* coupled to electrodes has been addressed only in Ref. [31], within a semiclassical model.

In this work, we investigate theoretically whether, and under what conditions, the spin-vibron coupling induces significant changes on the transport properties of a single-molecule nanomagnet coupled to spin-polarized electrodes (the system is sketched in Fig. 1). The numerical simulations reveal the effects of the vibron emission/absorption processes on the transient and stationary current, as well as on the electronic spin accumulation in the SMM. We focus on the transitions induced by the spin-vibron coupling between the fully polarized molecular configurations of spin $S_z = \pm(S + 1/2)$ and the next-nearest-neighbor excited states $S_z = \pm(S - 3/2)$, but the analysis could be extended to other transitions as well.

The calculations presented in this work complement our previous study on spin-vibron coupling effects on the transport properties of a nanoelectromechanical system (NEMS) with a grafted SMM [32]. Let us stress that in such an *indirect* transport setting [3,14,15], electrons do not tunnel through the molecular orbitals, and therefore the exchange interaction is expected to be rather small and its effect negligible; nonetheless, the theoretical study [33] considered such a coupling. More importantly, in the presence of the exchange interaction, the states of the composed system (i.e., the localized spin and the molecular orbital) cannot be described by a single pair of spin quantum numbers $\{s_z, S_z\}$ and they acquire a mixed structure.

The paper is organized as follows: in Sec. II we present the model and the transport formalism, Sec. III collects the numerical results, and Sec. IV is left for conclusions.

II. FORMALISM

In this work, the single-molecule magnet will be described by the so called giant-spin model [1], in which all constituting ions and the exchange and spin-orbit interactions between them are replaced by an effective Hamiltonian of a localized spin S. Detailed DFT analysis confirms that this model remains valid even in the presence of the electrodes [16].

A. The model Hamiltonian

The lowest electronic orbital of the SMM and its localized molecular spin are described by the Hamiltonian

$$H_{\rm SMM} = \sum_\sigma \epsilon_\sigma c_\sigma^\dagger c_\sigma + U\hat{n}_\uparrow\hat{n}_\downarrow - D\hat{S}_z^2 + E\left(\hat{S}_x^2 - \hat{S}_y^2\right) - \sum_i J_i \hat{s}_i \cdot \hat{S}_i + g\mu_B B\hat{S}_z^t. \quad (1)$$

In Eq. (1), ϵ_σ denotes the spin-degenerate energy of the lowest unoccupied molecular orbital, and $c_\sigma^\dagger$ (c_σ) are the corresponding creation (annihilation) operators. Also, $\hat{n}_\sigma = c_\sigma^\dagger c_\sigma$ is the number operator for electrons with spin orientation $\sigma = \uparrow, \downarrow$, and U is the Coulomb repulsion parameter. The electronic spin operators $\hat{s}_i$ $(i = x, y, z)$ are also expressed in terms of creation and annihilation operators as $\hat{s}_i = 1/2 \sum_{\sigma,\sigma'} c_\sigma^\dagger \sigma_{\sigma\sigma'}^i c_{\sigma'}$, where σ^i are the Pauli matrices.

Apart from its localized spin, the SMM is described by the easy-axis and transverse anisotropy terms. More precisely, D and E denote the anisotropy coefficients, and $\hat{S}_i$ are the components of the giant spin operator. Note that the z-component has eigenvalues S_z with quantum numbers $S_z = -S, \ldots, S$ such that $\hat{S}_z|S_z\rangle = S_z|S_z\rangle$. Additionally, the exchange interaction [i.e., the fifth term in Eq. (1)] induces simultaneous spin-flip processes for the electronic and molecular spins. In general, it is described by a tensor J_{ij}. As in other theoretical approaches [22,28], we shall neglect for simplicity the off-diagonal components and use the simplified notation $J_{ii} := J_i$. In this case, the exchange Hamiltonian reads

$$\sum_i J_i \hat{S}_i \hat{s}_i = \frac{J_-}{4}(\hat{S}_+\hat{s}_+ + \hat{S}_-\hat{s}_-) + \frac{J_+}{4}(\hat{S}_+\hat{s}_- + \hat{S}_-\hat{s}_+) + J_z\hat{S}_z\hat{s}_z, \quad (2)$$

where $\hat{S}_\pm = \hat{S}_x \pm i\hat{S}_y$ are jump operators for the molecular spin, and we introduced the coupling constants $J_\pm := J_x \pm J_y$. From Eq. (2) one infers that the simultaneous flip of the electronic and molecular spins is due to the transverse components of the exchange interaction J_x and J_y. The exchange coupling associated with the z-axis is spin-conserving and can only induce spin-dependent energy shifts (this feature is used in Ref. [26] to read the electronic spin from conductance measurements). In the isotropic case $J_x = J_y = J_z$, the above equation simplifies considerably [i.e., one is left only with

the second line of Eq. (2)]. Another intermediate regime is defined by $J_x = J_y \ll J_z$, and in particular the purely axial coupling corresponds to $J_x = J_y = 0$. This case, which does not allow for the spin-flip process, has been considered in a recent theoretical work [34].

The last term in Eq. (1) represents the Zeeman energy associated with a perpendicular magnetic field along the z-axis, and the total spin operator is given by $\hat{S}_z^t = \hat{S}_z + \hat{s}_z$; clearly, the eigenvalues of $\hat{S}_z^t$ are $m = -S - 1/2, \ldots, S + 1/2$. Finally, μ_B is the Bohr magneton and g is the gyromagnetic factor (we consider that $g = 2$).

In the following, we shall assume for simplicity that the electronic and molecular spins are coupled to a single quantized vibrational mode of frequency ω_0, with $a^\dagger$ and a being the harmonic-oscillator operators acting on the N-vibron Fock states $|N\rangle$. The electron-vibron coupling depends on the strength λ and on the local charge on the molecular orbital and is given by

$$H_{\text{el-vb}} = \lambda \sum_\sigma c_\sigma^\dagger c_\sigma (a^\dagger + a). \tag{3}$$

If the z-axis of the SMM is perpendicular to the direction of the electronic flow, the small torsional oscillations around this axis will induce a change of the transverse anisotropy term $E(\hat{S}_x^2 - \hat{S}_y^2)$ in Eq. (1) (see [1]). The corresponding spin-vibron coupling acquires the form [32,35]

$$H_{\text{sp-vb}} = -i\alpha E(\hat{S}_+^2 - \hat{S}_-^2)(a^\dagger + a), \tag{4}$$

and it shows that the vibron exchange involves molecular states whose spins differ by $\Delta S_z = \pm 2$. α denotes the dimensionless coupling strength. Then the Hamiltonian of the hybrid SMM-vibron system reads

$$\begin{aligned} H_S &= H_{\text{SMM}} + \hbar\omega_0 a^\dagger a + H_{\text{el-vb}} + H_{\text{sp-vb}} \\ &:= H_{S,0} + H_{\text{el-vb}} + H_{\text{sp-vb}}. \end{aligned} \tag{5}$$

The electron-vibron interaction can be eliminated by performing the well-known unitary Lang-Firsov (LF) transformation $U_{\text{LF}} = e^{\lambda/\hbar\omega_0 \hat{N}_S (a^\dagger - a)}$, where $\hat{N}_S = \sum_\sigma c_\sigma^\dagger c_\sigma$ is the total charge operator. The fermionic and bosonic operators transform as follows:

$$\tilde{c}_\sigma = U_{\text{LF}}^\dagger c_\sigma U_{\text{LF}} = c_\sigma e^{-\lambda(a^\dagger - a)/\hbar\omega_0} := c_\sigma \hat{\Lambda}, \tag{6}$$

$$\tilde{a} = U_{\text{LF}}^\dagger a U_{\text{LF}} = a + \frac{\lambda}{\hbar\omega_0}\hat{N}_S. \tag{7}$$

Then by straightforward manipulations one obtains the transformed Hamiltonian:

$$\tilde{H}_S = U_{\text{LF}}^\dagger H_S U_{\text{LF}} = \tilde{H}_{S,0} + H_{\text{sp-vb}}, \tag{8}$$

where

$$\tilde{H}_{S,0} = H_{S,0} - \lambda^2 \hat{N}_S/\hbar\omega_0 + 2i\frac{\lambda}{\hbar\omega_0}\alpha E(\hat{S}_+^2 - \hat{S}_-^2)\hat{N}_S. \tag{9}$$

Let us stress that the exchange term is quadratic in fermionic operators and therefore does not change under the LF transform. The last term in Eq. (9) arises from the LF transform of the spin-vibron term. It can be regarded as an additional transverse anisotropy coupling between the charged states, and it conserves the vibron number. However, we have checked that it brings negligible effects in the numerical calculations as long as $\alpha \ll \frac{\hbar\omega_0}{\lambda}$.

Since the Hamiltonian $\tilde{H}_{S,0}$ commutes with the vibron number operator $\hat{N}_V = a^\dagger a$, its eigenstates assume a factorized form $|\phi_{Q,\nu}; N\rangle = |\phi_{Q,\nu}\rangle|N\rangle$, where $|\phi_{Q,\nu}\rangle$ are the eigenfunctions of the renormalized SMM Hamiltonian $\tilde{H}_{\text{SMM}} := \tilde{H}_{S,0} - \hbar\omega_0 a^\dagger a$, and the index ν counts the available molecular states with electronic occupation $Q = 0, 1, 2$. There are $2S + 1$ empty molecular states (i.e., $Q = 0$) and $2(2S + 1)$ single-particle (or charged) states (i.e., $Q = 1$). We shall assume a strong Coulomb interaction U such that for a suitably chosen bias the double occupancy of the molecular orbital is forbidden. Then the two-electron states $|\phi_{2,\nu}; N\rangle$ will not contribute to the transport, and their explicit form is not needed here. The empty and charged states $|\phi_{Q,\nu}\rangle$ are expressed as linear combinations:

$$|\phi_{0,\nu}\rangle = \sum_{S_z} A_{S_z}^{(\nu)} |0, 0, S_z\rangle, \tag{10}$$

$$|\phi_{1,\nu}\rangle = \sum_{S_z,\sigma} B_{\sigma,S_z}^{(\nu)} |1, \sigma, S_z\rangle, \tag{11}$$

where $|Q = 0, s_z = 0, S_z\rangle$ denote the "empty" states with molecular spin S_z, and $|1, \sigma, S_z\rangle$ are the "single-charged" states of the Hamiltonian $\tilde{H}_{\text{SMM}}(J = 0, E = 0)$, $s_z = \pm 1/2$ being the projection of the electronic spin. In Eq. (11) it is understood that the spin orientations $\sigma = \uparrow, \downarrow$ correspond to the quantum numbers $s_z = \pm 1/2$.

The "delocalization" of the molecular spin of a state $|\phi_{Q,\nu}\rangle$ over more components $|S_z\rangle$ of the molecular spin is controlled by the coefficients $A_{S_z}^{(\nu)}$ and $B_{s_z,S_z}^{(\nu)}$. The empty molecular states contain only spin components with the same parity. For the single-particle states $|\phi_{1,\nu}\rangle$ this delocalization is due to *both* the exchange coupling and the transverse anisotropy term. If $E = 0$, the coefficients $B_{s_z,S_z}^{(\nu)}$ can be calculated analytically (see [21,24]). Note that the states $|Q, s_z, S_z\rangle$ contributing to $|\phi_{Q,\nu}\rangle$ are described by the same charge occupation Q. Therefore, the coefficients $A_{S_z}^{(\nu)}$ and $B_{\sigma,S_z}^{(\nu)}$ do not depend on Q.

To sum up, one has

$$\tilde{H}_{S,0}|\phi_{Q,\nu}, N\rangle = \mathcal{E}_{Q,\nu,N}|\phi_{Q,\nu}, N\rangle, \tag{12}$$

and the eigenvalues $\mathcal{E}_{Q,\nu,N}$ read

$$\mathcal{E}_{Q,\nu,N} = E_{Q,\nu} + N\hbar\omega_0, \tag{13}$$

where $E_{Q,\nu}$ is an eigenvalue of the LF transformed Hamiltonian $\tilde{H}_{\text{SMM}}$.

We shall now introduce a more convenient notation for the eigenfunctions $|\phi_{Q,\nu}\rangle$, which is valid as long as the magnetic field is chosen away from the degeneracy points $B = -D(S_z + S_z')/g\mu_B$ in the spectrum of $\tilde{H}_{\text{SMM}}(J = 0, E = 0)$. In this case, the mixing of the states $|0, 0, S_z\rangle$ induced by the transverse anisotropy is negligible, and one finds a majority spin component $\overline{S}_z$ such that the coefficients of the empty molecular states obey the condition $|A_{\overline{S}_z}^{(\nu)}|^2 \gg |A_{S_z'}^{(\nu)}|^2$ for all projections $S_z' \neq \overline{S}_z$. Consequently, there is a one-to-one correspondence between the index ν and the majority component $\overline{S}_z$ such that we can replace $|\phi_{0,\nu}\rangle \to |\phi_{\overline{S}_z}\rangle$, and as long as the transverse anisotropy effects are negligible one can approximate $|\phi_{\overline{S}_z}\rangle \approx |0, 0, \overline{S}_z\rangle$.

A similar argument holds for the single-electron states $|\phi_{1,\nu}\rangle$, the difference in this case being that the dominant component $\overline{m}$ refers to a specific value of the total spin quantum number S_z^t, such that one has $|B_{\overline{m}}^{(\nu)}|^2 \gg |B_{m'}^{(\nu)}|^2$ for any $m' \neq \overline{m}$. It is not difficult to check that the set of $2(2S+1)$ single-charged states $\{|\phi_{Q=1,\nu}\rangle\}$ can be labeled as $\{|\phi_{\overline{m}}^{\pm}\rangle, |\phi_{\pm(S+1/2)}\rangle\}$, where $\overline{m} = -S+1/2, \ldots, S-1/2$.

The states with spin $S_z^t = \pm(S+1/2)$ are not mixed by the exchange interaction, such that $|\phi_{S+1/2}\rangle = |1,\uparrow, S_z\rangle$ and $|\phi_{-S-1/2}\rangle = |1,\downarrow,-S_z\rangle$. For the intermediate states $|\phi_{\overline{m}}^{\pm}\rangle$ it turns out that in the expansion given by Eq. (11) there are only *two* coefficients associated with a dominant total magnetic number $\overline{m}$ such that one can write

$$|\phi_{\overline{m}}^{\pm}\rangle \approx B_{\downarrow,\overline{m}+1/2}^{\pm}|1,\downarrow,\overline{m}+1/2\rangle + B_{\uparrow,\overline{m}-1/2}^{\pm}|1,\uparrow,\overline{m}-1/2\rangle. \tag{14}$$

The last equation also shows that the majority spin components of the empty and single-charged states have different parities. We shall also use the new notation for the corresponding eigenvalues of the LF-transformed Hamiltonian $\tilde{H}_{\rm SMM}$, more precisely $E_{0,\nu} \to E_{\overline{S}_z}$ and $\{E_{1,\nu}\} \to \{E_{\overline{m}}^{\pm}, E_{\pm(S+1/2)}\}$, where the index $\pm$ of the energy branches is assigned such that $E_{\overline{m}}^{+} > E_{\overline{m}}^{-}$. These eigenvalues cannot be calculated analytically unless the anisotropy term vanishes (i.e., $E=0$). In that case, the total molecular m spin is conserved and one has (see Ref. [24])

$$E_m^{\pm} = \epsilon_\sigma + g\mu_B B m + \frac{J}{4} - D\left(m^2+\frac{1}{4}\right) \pm \Delta E(m), \tag{15}$$

where $\Delta E(m) = [D(D-J)m^2 + (J/4)^2(2S+1)^2]^{1/2}$. This expression could still be used as a good approximation as long as the ratio $E/D \ll 1$. In particular, it suggests that the eigenvalues of $\tilde{H}_{\rm SMM}$ acquire Zeeman shifts which depend on the dominant molecular component $\overline{m}$. Equation (15) also shows that, when represented as a function of the dominant quantum number $\overline{m}$, each energy branch defines a parabola and a corresponding anisotropy barrier. The energies of the empty molecular states $E_{\overline{S}_z} \approx -D\overline{S}_z^2 + g\mu_B B\overline{S}_z$ lie as well on a parabola.

The same simplified notation applies to the eigenvalues of $\tilde{H}_{S,0}$, which are now written as follows:

$$\mathcal{E}_{\overline{S}_z,N} = E_{\overline{S}_z} + N\hbar\omega_0, \quad \mathcal{E}_{\overline{m}}^{\pm} = E_{\overline{m}}^{\pm} + N\hbar\omega_0. \tag{16}$$

Finally, the eigenfunctions $|\psi_{Q,j}\rangle$ of $\tilde{H}_S$ can be found by numerical diagonalization, by truncating the number of vibronic states to N_0. Note that the spin-vibron coupling allows only the conservation of the electronic charge Q on the molecular orbital, whereas the electronic and molecular spins, as well as the vibron number, are no longer conserved. The eigenstates $|\psi_{Q,j}\rangle$ are then written as linear combinations of "free" states of $\tilde{H}_{S,0}$:

$$|\psi_{Q=0,j}\rangle = \sum_{\overline{S}_z,N} C_{\overline{S}_z,N}^{(j)}|\phi_{\overline{S}_z};N\rangle, \tag{17}$$

$$|\psi_{Q=1,j}\rangle = \sum_{\overline{m},N,p=\pm} C_{\overline{m},N,p}^{(j)}|\phi_{\overline{m}}^{p};N\rangle. \tag{18}$$

In Eq. (18) the branch index $p=\pm$ if $\overline{m}$ corresponds to the intermediate states and is absent for the fully spin-polarized states with $\overline{m} = \pm(S+1/2)$.

B. The transport setting

The single-molecule magnet is connected to source (left) and drain (right) leads described as noninteracting particle reservoirs with chemical potentials $\mu_{L,R}$ (see Fig. 1). The Hamiltonian of the open system reads

$$H(t) = \tilde{H}_S + H_L + \tilde{H}_T(t), \tag{19}$$

where $\tilde{H}_T$ is the tunneling Hamiltonian in which the creation and annihilation operators were transformed according to Eq. (6) and H.c. denotes the Hermitian conjugate:

$$\tilde{H}_T(t) = \sum_{\alpha=L,R}\sum_{\sigma}\int_0^{\pi} dq_\alpha \chi_\alpha(t)(V_\alpha^\sigma c_\sigma^\dagger \Lambda^\dagger c_{q_\alpha\sigma} + \text{H.c.}). \tag{20}$$

The parameter V_α^σ is the hopping amplitude between the orbital level of the SMM with energy ϵ_σ and the electronic spin states in the lead α with momentum q_α. We assumed spin-conserving tunneling processes, that is, the electron does not flip its spin when tunneling between the molecule and the particle reservoirs. Then we denote $V_\alpha^\uparrow = V_\alpha^\downarrow := V_\alpha$. In the tight-binding representation of the leads that we use here, one obtains a simple expression for the energy of the incident electron, that is, $\varepsilon_q = 2t_L\cos q$ (with t_L being the hopping constant on the leads). Note that the Hamiltonian H_L of the noninteracting leads does not change under the LF transformation.

In the partitioning approach to quantum transport [36,37], the two switching functions $\chi_{L,R}(t)$ simulate the coupling of the nanomagnet to the leads. For simplicity, we consider that the coupling to the leads is established at instant $t=0$ and that $\chi_{L,R}(t) = \theta(t)$, where $\theta(x)$ is the step function.

The spin polarization of the lead α is defined as

$$P_\alpha^\sigma := \left(N_\alpha^\sigma - N_\alpha^{\overline{\sigma}}\right)/\left(N_\alpha^\sigma + N_\alpha^{\overline{\sigma}}\right), \tag{21}$$

where N_α^σ and $N_\alpha^{\overline{\sigma}}$ are the density of states for the majority (σ) and minority ($\overline{\sigma}$) spin in the lead α. We shall use this notation to introduce various spin-polarized configurations of the leads. We consider that the two leads have the same total density of states N_D, that is, $N_\alpha^\uparrow + N_\alpha^\downarrow = N_D$. If $N_\alpha^\uparrow = 0$, the lead α is magnetic (i.e., fully polarized) and carries only spin-down electrons, i.e., $P_\alpha^\downarrow = 1$. Partially polarized leads are defined by intermediate polarizations $P_\alpha^\sigma \in (0,1)$. In addition, a nonmagnetic lead is described by equal spin densities, that is, $N_\alpha^\uparrow = N_\alpha^\downarrow$, from where it follows that $P_\alpha^\uparrow = P_\alpha^\downarrow = 0$.

Within the Markov approximation, the master equation for the reduced density operator ρ of the hybrid system takes the form (see Ref. [37])

$$\dot{\rho}(t) = -\frac{i}{\hbar}[\tilde{H}_S, \rho(t)] - \mathcal{L}_{\rm leads}[\rho(t)] - \mathcal{L}_\kappa[\rho(t)], \tag{22}$$

where $\mathcal{L}_{\rm leads}$ takes into account the contribution of the particle reservoirs (i.e. the leads):

$$\mathcal{L}_{\rm leads} = \frac{1}{\hbar^2}\int_0^\infty ds \,\text{Tr}_{\rm leads}\{[\tilde{H}_T, [\tilde{H}_{T,I}(-s), \rho(t)\rho_{\rm leads}]]\}, \tag{23}$$

where $\mathrm{Tr}_{\mathrm{leads}}\{\cdot\}$ denotes the partial trace with respect to the leads, ρ_{leads} is their equilibrium statistical operator, and $\tilde{H}_{T,I}(t)$ stands for the interaction picture with respect to the unitary evolution of the decoupled Hamiltonian, that is, $\tilde{H}_{T,I}(t) = e^{\frac{i}{\hbar}t\tilde{H}_S}e^{\frac{i}{\hbar}tH_L}\tilde{H}_T e^{-\frac{i}{\hbar}t\tilde{H}_S}e^{-\frac{i}{\hbar}tH_L}$. For computational purposes, one has to replace the two tunneling Hamiltonians in Eq. (23) and then generate several terms associated with various tunneling-in or -out processes. For example, the tunneling of an electron with spin σ from the electrode α to the molecular orbital changes the configuration of the SMM from an empty molecular state $|\psi_{Q=0,j}\rangle$ to a charged state $|\psi_{Q=1,j'}\rangle$. Using the fully interacting basis of $\tilde{H}_S$, one finds that the corresponding term in the Lindblad equation is (see Ref. [32])

$$T_{\alpha\sigma,j'j} = f_\alpha(\tilde{\mathcal{E}}_{1,j'} - \tilde{\mathcal{E}}_{0,j})\sqrt{N_\alpha^\sigma}V_\alpha\langle\psi_{1,j'}|c_\sigma^\dagger\Lambda^\dagger|\psi_{0,j}\rangle. \quad (24)$$

The last term $\mathcal{L}_\kappa$ in the master equation describes the dissipation processes due to a thermal reservoir, n_B being the Bose-Einstein distribution. The Lang-Firsov transformation leads to the following form of $\mathcal{L}_\kappa$ [38]:

$$\mathcal{L}_\kappa\rho(t) = (n_B+1)\mathcal{D}_\kappa[a]\rho(t) + n_B\mathcal{D}_\kappa[a^\dagger]\rho(t) + \left(\frac{\lambda}{\hbar\omega_0}\right)^2(2n_B+1)\mathcal{D}_\kappa[\hat{N}_S]\rho(t), \quad (25)$$

where we introduced the notation

$$\mathcal{D}_\kappa[X]\rho(t) = \frac{\kappa}{2}(X^\dagger X\rho + \rho X^\dagger X - 2X\rho X^\dagger), \quad (26)$$

and the operator $X = a, a^\dagger, \hat{N}_S$. The master equation is solved with respect to the basis of fully interacting states $\{\psi_{Q,j}\}$, while the statistical averages can be also calculated with respect to the basis of $\tilde{H}_{S,0}$, using the unitary transformation which connects it to the fully interacting basis [see Eqs. (17) and (18)]. It is also useful to discuss the occupation of the molecular configurations with dominant spin components $\overline{S}_z$ and $\overline{m}$, calculated by collecting the contributions from the N-vibron states $|\phi_{\overline{S}_z,N}\rangle$ and $|\phi_{\overline{m},N}\rangle$. For example, the population of the intermediate single-particle state $|\phi_{\overline{m}}^\pm\rangle$ is calculated as

$$P_{\overline{m}}^\pm(t) = \sum_N\langle\phi_{\overline{m}}^\pm;N|\rho(t)|\phi_{\overline{m}}^\pm;N\rangle := \sum_N P_{\overline{m},N}^\pm(t). \quad (27)$$

Note that the integer and half-integer values of $\overline{m}$ distinguish between the empty and charged SMM states. The statistical average of the localized spin is calculated as

$$\langle S_z\rangle(t) = \mathrm{Tr}\{\rho(t)\hat{S}_z\}, \quad (28)$$

where the trace is taken over all states of the hybrid system. Similarly, one can compute the average number of vibrons $\langle N_V\rangle(t) := \mathrm{Tr}\{\rho(t)a^\dagger a\}$ and the total electronic charge $\mathcal{Q}_S = \mathrm{Tr}\{\rho(t)e\hat{N}_S\}$ (e denotes the electron charge). The time-dependent currents $J_{L,R}$ in the two leads are identified from the continuity equation:

$$\frac{d}{dt}\mathcal{Q}_S(t) = e\mathrm{Tr}\left\{\hat{N}_S\frac{d}{dt}\rho(t)\right\} = J_L(t) - J_R(t). \quad (29)$$

In the long-time limit, the system evolves towards a stationary state characterized by the stationary current $J_L = J_R := J_S$. Let us point out that most studies on transport through single-molecule magnets rely on stationary Markovian master equations (see Refs. [11,18,30,33]). Markovian calculations for a system of N spins on a metallic surface were also presented in Ref. [39]. Notably, this system is described by the Lipkin-Meshkov-Glick (LMG) model [40]. However, to capture the information backflow in helical quantum rings coupled to non-Markovian magnonic baths, one has to rely on alternative methods [41].

III. NUMERICAL RESULTS AND DISCUSSION

Let us consider a single-molecule magnet described by a localized spin $S = 2$. For the numerical simulation we used $D = 0.056$ meV, corresponding to a rather small anisotropy energy barrier $DS^2 = 0.224$ meV. The transverse anisotropy coefficient E is fixed by the ratio $E/D = 1/15$, and the exchange interaction is assumed to be isotropic, $J_x = J_y = J_z := J$, with the strength $J = 0.25$ meV. The electron-vibron and spin-vibron coupling strengths are set to $\lambda = 0.5$ meV and $\alpha = 0.15$. The energy of the spin-degenerate molecular orbital $\epsilon_\uparrow = \epsilon_\downarrow := \epsilon_0$ can be conveniently tuned by a gate voltage; the calculations were performed for $\epsilon_0 = 1$ meV. The loss coefficient is $\kappa = 0.05$ μeV, and the temperature of the environment is $T = 50$ mK. The strength of the Coulomb interaction is set to $U = 2.5$ meV.

The Markovian master equation is solved numerically by taking into account up to $N_0 = 15$ vibron states. We found that this cutoff ensures the convergence of the numerical results, that is, the mean vibron number, the current, and the average molecular spin do not change significantly when N_0 increases.

A. Removal of the spin blockade

In this section, we consider that the left electrode provides only spin-down electrons (i.e., $P_L^\downarrow = 1$), while the right (i.e., drain) electrode carries mostly spin-up electrons, that is, $N_R^\uparrow > N_R^\downarrow$. This quasi-antiparallel configuration, denoted in the following by $\downarrow_L\uparrow_R$, is also depicted in Fig. 1; the fully antiparallel configuration corresponds to $P_L^\downarrow = P_R^\uparrow = 1$. The numerical simulations were performed for the initial density matrix $\rho(t=0) = |\phi_{-2};0\rangle\langle\phi_{-2};0|$, which corresponds to the lowest energy of the system. We emphasize here that the constant perpendicular magnetic field along the z-axis leads to Zeeman shifts and removes the degeneracy between the lowest doublet with spins $S = \pm 2$. Therefore, the transverse anisotropy induces a negligible mixing of the empty molecular states, since $E \ll D$. The chemical potentials of the electrodes are $\mu_L = 3$ meV and $\mu_R = -3$ meV; for these values, the double occupancy of the LUMO is forbidden.

In the absence of the spin-vibron coupling, the energies of the empty and charged molecular states of $\tilde{H}_{S,0}$ [see Eq. (16)] can be represented as points lying on different parabolas as a function of their integer ($\overline{S}_z$) and half-integer ($\overline{m}$) dominant spin components. Three such branches are shown in Fig. 2: the lowest inverted parabola corresponds to $\mathcal{E}_{\overline{S}_z,N}$, the other to charged molecular energy levels $\mathcal{E}_{\overline{m},N}^+$ and $\mathcal{E}_{\overline{m},N+1}^+$. The lowest energy branch $\mathcal{E}_{\overline{m},N}^-$ is not represented.

First, it is not difficult to observe that the energy gaps between the next-nearest-neighbor levels $E_{-1/2}^\pm$ and $E_{-5/2}$ have a linear dependence on the transverse magnetic field; this feature is also predicted by the Zeeman terms in Eq. (15).

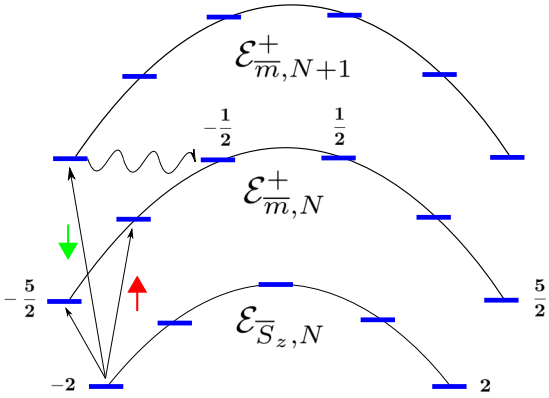

FIG. 2. Energy branches, sequential tunneling processes (black arrows), and vibron-assisted transitions on the left side of the anisotropy barrier for a SMM described as localized spin $S = 2$. The spins involved in the tunneling processes are represented with colored arrows. The wavy line indicates vibron-assisted transitions associated with the resonant condition $\mathcal{E}_{-5/2,N+1} = \mathcal{E}^{+}_{-1/2,N}$.

Secondly, since $\mathcal{E}_{-5/2,N+1} - \mathcal{E}^{\pm}_{-1/2,N} = E_{-5/2} - E^{\pm}_{-1/2} + \hbar\omega_0$, one expects that the spin-vibron coupling induces vibron-assisted transitions between the states $|\phi_{-5/2}; N+1\rangle$ and $|\phi^{\pm}_{-1/2}; N\rangle$ as the magnetic field sweeps the resonant values $\hbar\omega_0 = E^{\pm}_{-1/2} - E_{-5/2}$. These transitions should play a role both in the population dynamics and in transport. In this section, we shall focus on the vibron-assisted transitions associated with the positive energy branch. Taking into account the calculated values of $E^{+}_{-1/2}$ and $E_{-5/2}$, we set the frequency of the vibrational mode to $\hbar\omega_0 = 0.85$ meV [42].

The resonant condition $\mathcal{E}_{-5/2,N+1} = \mathcal{E}^{+}_{-1/2,N}$ is expected to enhance the role of the spin-vibron coupling. As a consequence, the leftmost fully spin-polarized state $|\phi_{-5/2}, N+1\rangle$ and the intermediate state $|\phi^{+}_{-1/2}, N\rangle$ turn into a pair of vibron-dressed states [see Eq. (18)]. In Fig. 3(a) we plot the magnetic field dependence of the energies corresponding to four such dressed states of the fully interacting Hamiltonian $\tilde{H}_S$. The energy spectrum showed in Fig. 3(a) has features encountered in the Jaynes-Cummings (JC) model in quantum optics [43,44]: (i) at some value of the magnetic field (i.e., $B = 150$ mT), there is an avoided crossing point for each pair of energies; (ii) the energy gap at the resonance point increases with the vibron number N; and (iii) the spectral branches for $N = 0$ and 1 are roughly separated by the single-vibron energy $\hbar\omega_0$.

Figure 3(b) also shows the weights of the "free" states $|\phi_{-5/2}, 1\rangle$ and $|\phi^{+}_{-1/2}, 0\rangle$ in the lowest-energy dressed state. Again, as in the JC model, these weights vary smoothly between 0 and 1, being nearly equal at resonance. Obviously, far away from the avoided crossing point (i.e., in the off-resonant regime) one recovers the "free" states and their corresponding eigenvalues $\mathcal{E}_{-5/2,N=1,2}$ and $\mathcal{E}^{+}_{-1/2,N=0,1}$ [indicated in Fig. 3(a)] as the spin-vibron coupling becomes inactive. Let us stress that the charged states $|\phi^{\pm}_{\overline{m}}, N\rangle$ with dominant molecular spin $\overline{m} \neq -5/2, -1/2$ are *not* mixed by the spin-vibron coupling. Nonetheless, they contribute significantly to the transport process.

For example, the black arrows in Fig. 2 indicate tunneling processes between the empty state $|\phi_{-2}; N\rangle$ and the neighbor single-charged states $|\phi_{-5/2}; N'\rangle$ and $|\phi^{+}_{-3/2}; N'\rangle$, where

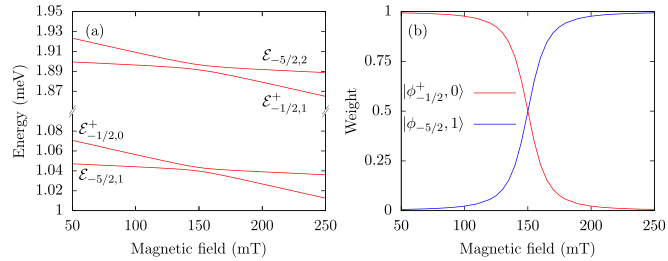

FIG. 3. (a) The magnetic field dependence of the $N = 0$ and 1 energy doublets associated with pairs of dressed states made of $|\phi_{-5/2}, N+1\rangle$ and $|\phi^{+}_{-1/2}, N\rangle$ "free" states. (b) The weights of the "free" states in the lowest-energy dressed state.

$N' = N, N+1$. It is clear that $|\phi_{-2}; N\rangle$ and $|\phi_{-5/2}; N'\rangle$ are connected by tunneling of spin-down electrons. Then, tunneling-in processes lead to heating if $N' > N$, while for vibron emission associated with tunneling-out events one has $N' < N$. Vibron absorption processes (i.e., cooling) are defined in a similar way. The number of vibrons emitted in the tunneling processes depends on the chemical potentials of the leads. In fact, we find that the energy spectra of the Hamiltonians $\tilde{H}_S$ and $\tilde{H}_{S,0}$ [see Eqs. (8) and (9)] are quite close. Then from Eq. (24) it follows that the emission of $(N' - N)$ vibrons requires that $\mu_\alpha > \mathcal{E}_{-5/2,N'} - \mathcal{E}_{-2,N}$. Also, corroborating the mixed spin structure of the intermediate states [i.e., $|\phi^{\pm}_{-3/2}\rangle \approx B^{\pm}_{\downarrow,-1}|1,\downarrow,-1\rangle + B^{\pm}_{\uparrow,-2}|1,\uparrow,-2\rangle$—see Eq. (14)] and the spin selection rules, one infers that they can be populated only by tunneling of a spin-up electron from the left contact.

It is important to observe that in the off-resonant regime, electrons are allowed to tunnel only to the state $|\phi_{-5/2}; N\rangle$, while the excited molecular states $|\phi^{\pm}_{-3/2}; N\rangle$ are not available. This happens because the fully polarized left electrode prevents the tunneling process involving the component $|Q = 1, \sigma = \uparrow, S_z = -2\rangle$ of the charged states $|\phi^{\pm}_{-3/2}; N\rangle$. Moreover, the molecular spin is pinned to $S_z = -2$ due to the selection rules for tunneling. In other words, the antiparallel configuration $\downarrow_L\uparrow_R$ does not allow the climbing of the anisotropy barrier in the off-resonant regime and also imposes a simultaneous blockade on the electronic and molecular spins. Note, however, that electrons tunnel to the drain electrode by the depletion of the state $|\phi_{-5/2}; N\rangle$, as long as $P^{\uparrow}_R < 1$.

In Fig. 4(a), we present the steady-state current as a function of the magnetic field and for several polarizations $P^{\uparrow}_R$ of the drain electrode. As stated above, in the off-resonant regime the current is due to the cumulative "background" contribution of the N-vibron states $|\phi_{-5/2}; N\rangle$ and shows only a weak dependence on the magnetic field. As one enters the resonant regime, a symmetric peak develops for all values of $P^{\uparrow}_R$. The height of these peaks decreases if the polarization $P^{\uparrow}_R$ is reduced, whereas the background off-resonant current increases. This amplification of the stationary current in the resonant regime could be observed in typical transport measurements and witnesses the activation of the spin-vibron coupling and the corresponding transitions. Let us note that the difference between the off-resonant and resonant stationary currents is sizable [for $P^{\uparrow}_R = 0.7$ it goes up to 15 pA—this is better seen in Fig. 5(a) below].

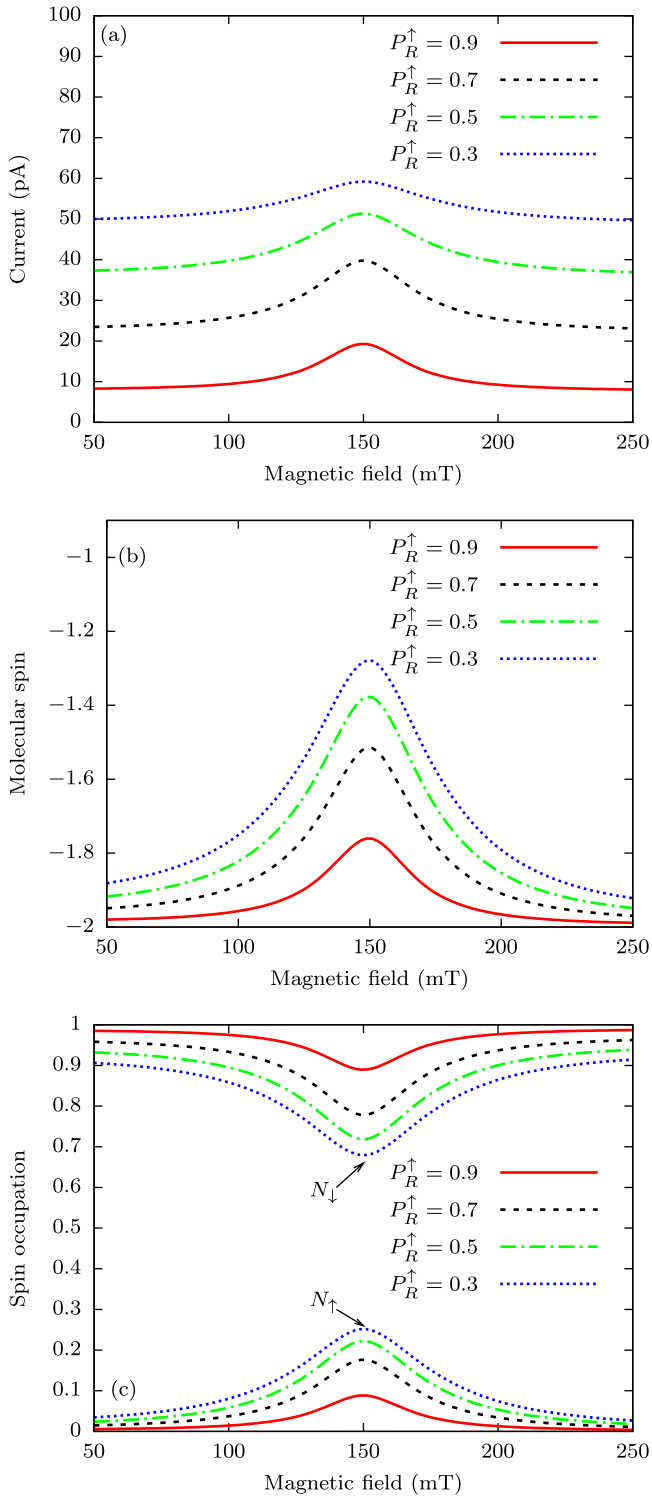

FIG. 4. (a) The stationary current J_S as a function of the magnetic field. (b) The average molecular spin. (c) The spin occupations $N_\uparrow$ and $N_\downarrow$. The removal of the spin blockade around the resonance point $B = 150$ mT coincides with the enhancement of charge transport. The amplitude of the correlated peaks of the current and molecular spin depends on the spin polarization $P_R^\uparrow$ in the right electrode. Other parameters: $V_L = 25$ μeV, $V_L = 10$ μeV.

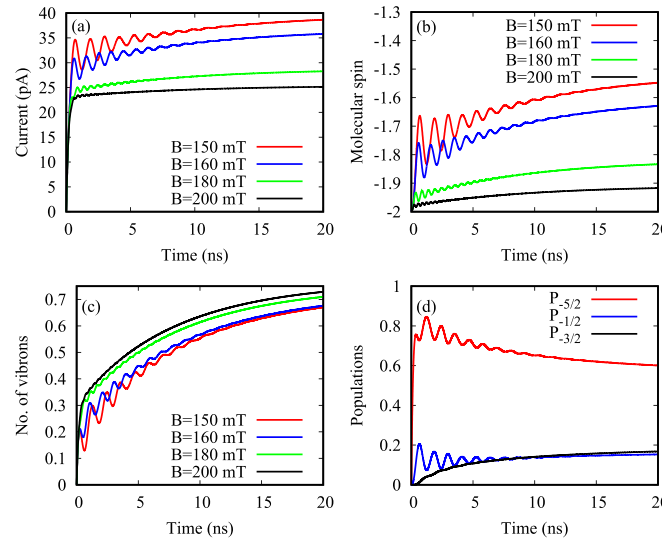

FIG. 5. (a) The transient current $J_R(t)$ for several values of the magnetic field. (b) The short-time dynamics of the molecular spin $\langle S_z\rangle(t)$. (c) The vibron number $\langle N_V\rangle(t)$. (d) The time-dependent populations of relevant charged configurations in the resonant regime (i.e., for $B = 150$ mT). Other parameters: $P_R^\uparrow = 0.7$, $V_L = 25$ μeV, $V_R = 10$ μeV.

The dependence of the stationary average molecular spin $\langle S_z\rangle$ on the magnetic field is shown in Fig. 4(b). One notices the removal of the spin blockade in the resonant regime. More precisely, around resonance $\langle S_z\rangle$ displays a series of peaks as a function of $P_R^\uparrow$, while in the off-resonant regime $\langle S_z\rangle \approx -2$. The obvious correspondence between the peaks in Figs. 4(a) and 4(b) also allows the reading of changes in the molecular spin from the enhancement of the stationary current in the resonant or nearly resonant regime. The increase of the molecular spin at the resonance point indicates that excited molecular states with dominant spin number $|\overline{m}| < 2$ must come into play. As for the mean vibron number $\langle N_V\rangle$, we find that a smooth dip develops as the magnetic field sweeps the resonant value (not shown).

Now let us discuss the electronic spin accumulation in the SMM. From Fig. 4(c) one notices that away from resonance the occupation $N_\uparrow$ of the spin-up state almost vanishes if the drain electrode is highly polarized (i.e., for $P_R^\uparrow = 0.9$ and 0.7). Conversely, $N_\downarrow \approx 1$, because the depletion of the spin-down electron is strongly prohibited. As the system approaches the resonant regime, the electronic spin blockade is lifted. More precisely, $N_\uparrow$ reaches a maximum on resonance for all values of $P_R^\uparrow$, while $N_\downarrow$ develops a dip that is enhanced as $P_R^\uparrow$ decreases. Note that if $P_R^\uparrow = 1$, the molecular orbital is fully occupied and the stationary current vanishes (not shown).

Additional information on the spin-vibron effects is also provided by the transient currents, which are presented in Fig. 5(a) for several values of the magnetic field and $P_R^\uparrow = 0.7$. The transient current displays Rabi oscillations that are more pronounced at resonance (i.e., for $B = 150$ mT) and almost disappear in the off-resonant regime (e.g., for $B = 200$ mT).

Even in the resonant case, the oscillations are damped by the tunneling processes, which act as dissipative channels. It is important to emphasize here the role of the asymmetric coupling to the leads, $V_L > V_R$. In this case, the tunneling rate to the drain electrode decreases and favors the observation of several Rabi oscillations. Although for symmetric coupling we find fewer oscillations, the changes of the stationary currents when passing through the resonance point remain important.

Figure 5(b) shows that around resonance, the average molecular spin also develops oscillations; in contrast, away from resonance, the spin evolves smoothly towards the steady-state value. We find similar damped oscillations for the average vibron number [see Fig. 5(c)]. These oscillations are clearly associated with absorption and emission of vibrons during molecular spin transitions between states $|\phi_{-5/2}; N+1\rangle$ and $|\phi^{+}_{-1/2}; N\rangle$. On the other hand, the smooth increase of $\langle N_V \rangle$ towards the stationary regime reflects the heating of the system via tunneling processes. In Figs. 5(a)–5(c) one notices that the oscillation period decreases as the magnetic field varies. This behavior is again explained in the framework of the JC model, which predicts that the period of the Rabi oscillation decreases as a function of the detuning, $E^{+}_{-1/2} - E_{-5/2} - \hbar\omega_0$.

The time-dependent populations of the single-particle spin configurations which participate to transport in the resonant regime are displayed in Fig. 5(d). Each population collects contributions from all vibrational states, as indicated in Eq. (27). Note that for $\overline{m} = -3/2, -1/2$ we represent the total occupation, $P_{\overline{m}}(t) = P^{+}_{\overline{m}}(t) + P^{-}_{\overline{m}}(t)$. Both $P_{-5/2}$ and $P_{-1/2}$ exhibit Rabi oscillations in the early transient regime, confirming once again the presence of the spin transitions induced by the spin-vibron coupling. We have checked that the population of the states $|\phi^{-}_{-1/2}; N\rangle$ does not exhibit oscillations, as the corresponding energies are detuned. In contrast, $P_{-3/2}$ only emerges at some later times and increases uniformly. We stress that in the off-resonant regime (e.g., for $B = 250$ mT), $P_{-3/2}$ and $P_{-1/2}$ are vanishingly small (not shown), while $P_{-5/2}$ does not develop Rabi oscillations. Now, each of the single-particle states $|\phi^{\pm}_{\overline{m}}; N\rangle$ with $\overline{m} = -3/2, -1/2$ is coupled to empty molecular states via sequential tunneling-in or -out processes. For instance, the depletion of the states with $\overline{m} = -1/2$ and $-3/2$ is mostly due to spin-up tunneling processes to the right electrode. This leads in turn to nonvanishing populations of the empty molecular states $|\phi_{-1}\rangle$ and $|\phi_{-2}\rangle$ both in the transient and stationary regimes (not shown). Also, by looking at the spin structure of the single-particle states, one infers that the "chain" of sequential tunneling processes leading to magnetic switching cannot be completed. Indeed, we find that configurations with molecular spin $\overline{m} > 0$ are not available, because spin polarization of the left electrode does not allow the tunneling-in process of spin-up electrons $|\phi_0\rangle \to |\phi^{\pm}_{1/2}\rangle$. This also explains why at resonance the stationary average value of the molecular spin goes only up to $\langle S_z \rangle \approx -1.5$ [see Fig. 4(b)].

The analysis presented in this section proves that the unpinning of the electronic spin and the amplification of the stationary current in the resonant regime result from the interplay of the spin-vibron and the exchange interaction. The former allows resonant transitions to the excited states $|\phi^{+}_{-1/2}; N\rangle$, whereas the latter imposes the mixed spin structure of this state, according to Eq. (14). As shown in Fig. 5(d), the increase of the spin-up occupation $N_\uparrow$ is clearly related to the activation of more excited states with energies on the left side of the anisotropy barrier. On the other hand, these states allow the tunneling of *both* spins to the drain electrode. Therefore, the resonant transitions activate additional transport channels which add up to the off-resonant background current. Let us stress that all these processes are also active when the left lead is nonmagnetic (i.e., if $P^{\uparrow}_L = P^{\downarrow}_L = 0$). In this case, the spin blockade is not set and the states $|\phi^{\pm}_{-3/2}, N\rangle$ are populated even in the off-resonant regime. This reduces the visibility of the Rabi oscillations in the transient current.

B. Current-induced magnetic switching

In this subsection, we shall consider that the left electrode injects only spin-up electrons (i.e., $P^{\uparrow}_L = 1$), while the right electrode carries mostly spin-down electrons, such that $P^{\downarrow}_R > 0$. This configuration, denoted by $\uparrow_L\downarrow_R$, prevents the tunneling to the fully spin-polarized state $|\phi_{-5/2}\rangle$ and allows the occupation of the states $|\phi^{\pm}_{-3/2}\rangle$. On the other hand, the dominant depletion of the spin-down electrons to the right electrode favors the empty molecular states with increasing spin. In the steady-state regime, this sequence of tunneling processes ends up in current-induced magnetic switching $S \to -S$, such that the system is described only by the fully polarized states $|\phi_{5/2}\rangle$ and $|\phi_2\rangle$ (see Ref. [24]).

We stress that the magnetic switching is due to the exchange interaction between the electronic and molecular spins, which causes a strong mixing of the states $|Q = 1, \sigma, S_z\rangle$. Since the electron-vibron coupling conserves both the electronic and molecular spins, one expects that the same switching mechanism should still be at work if $\lambda \neq 0$.

To check the effect of the spin-vibron interaction in the $\uparrow_L\downarrow_R$ configuration, we select a frequency of the vibrational mode which activates transitions on the right side of the anisotropy barrier, namely between the fully polarized states $|\phi_{5/2}; N\rangle$ and the excited molecular states $|\phi^{+}_{1/2}; N-1\rangle$. For $B = 150$ mT and $J = 0.25$ meV we find that the resonant frequency of the vibrational mode is given by $\hbar\omega_0 = E^{+}_{1/2} - E_{5/2} = 0.78$ meV. In this section, we consider symmetric coupling to the leads, $V_L = V_R = 25$ μeV, while keeping $\mu_L = 3$ meV and $\mu_R = -3$ meV.

Transport calculations were performed for different polarizations $P^{\downarrow}_R$ of the right electrode. In fact, the values of $P^{\downarrow}_R$ are varied from the nonmagnetic case ($P^{\downarrow}_R = 0$) to the fully spin-down polarization $P^{\downarrow}_R = 1$. The transient currents in the resonant ($B = 150$ mT) and off-resonant ($B = 300$ mT) regimes are shown in Fig. 6(a). A clear enhancement of the stationary current is noticed in the resonant case. More precisely, the *difference* between the resonant and off-resonant stationary currents increases from 50 pA for $P^{\uparrow}_R = 0.4$ to almost 80 pA for $P^{\uparrow}_R = 0.7$. Also, the transient currents show that the evolution towards the steady-state regime is faster in the presence of molecular spin transitions. In the resonant case, the currents reach a constant value around $t = 5$ ns, whereas in the off-resonant regime a longer time is needed (i.e., $t \approx 15$ ns).

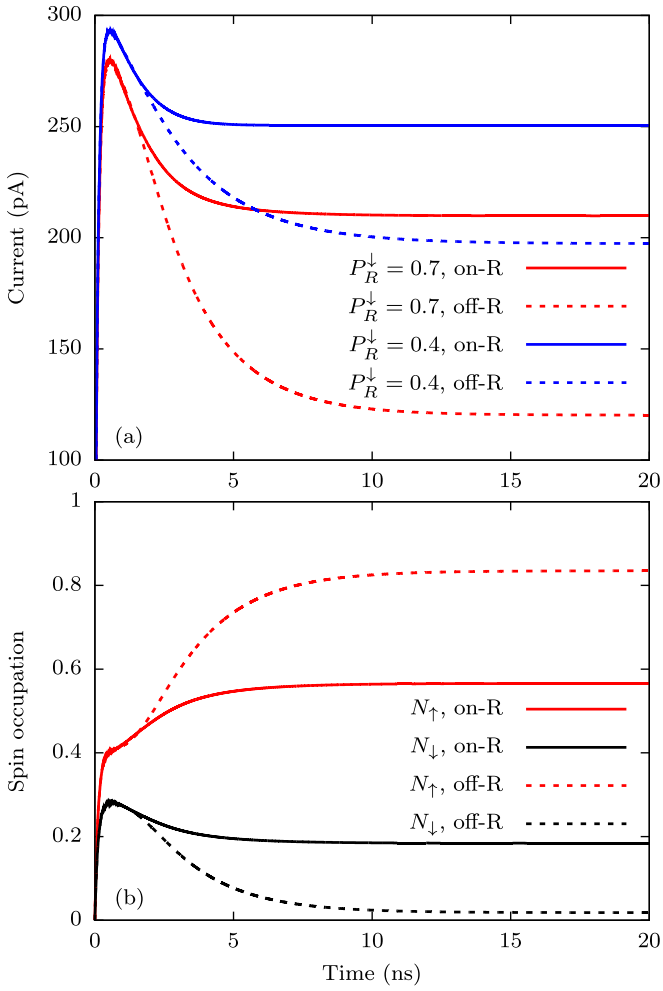

FIG. 6. (a) The transient currents $J_R(t)$ for two values of the polarization $P_R^\downarrow$ in the resonant regime (on-R), solid lines; and the off-resonant regime (off-R), dashed lines. (b) The spin-dependent electronic occupations in the resonant and off-resonant regimes for $P_R^\downarrow = 0.7$.

Figure 6(b) illustrates the effects of the spin-vibron coupling on the spin-dependent electronic occupations N_σ. In both resonant and off-resonant cases, the spin accumulation is much faster up to $t \sim 1.5$ ns, and it corresponds to the abrupt increase of the transient currents in Fig. 6(a). Then the evolution of the spin occupations displays fingerprints of the vibron-assisted transitions. In the off-resonant regime, the orbital is spin-up polarized (i.e., $N_\downarrow \approx 0$) but not fully occupied ($N_\uparrow \approx 0.82$); this happens because in the stationary regime the tunneling process involves only the fully polarized state $|\phi_{5/2}\rangle = |Q = 1, \uparrow, S_z = 2\rangle$. When the spin-vibron coupling comes into play, the spin-down occupation no longer vanishes whereas the spin-up occupation decreases considerably. Also, the total charge occupation $N_\uparrow + N_\downarrow$ decreases in the resonant regime, which explains the current enhancement seen in Fig. 6(a). Since the state $|\phi_{5/2}\rangle$ is spin-up polarized, the accumulation of spin-down electrons suggests that other intermediate molecular states participate to transport in the resonant regime.

Let us stress that in this antiparallel configuration of the electrodes there are no visible Rabi oscillations of the transient currents. Nonetheless, the results in Fig. 6 show that the spin-vibron coupling still imposes sizable changes on the stationary transport properties. To explain these features, we recall that at resonance (or close to it) the pairs of states $\{|\phi_{5/2}; N\rangle, |\phi^+_{1/2}; N-1\rangle\}$ merge into "dressed" states. This mixed structure implies nonvanishing occupations of the state $|\phi^+_{1/2}, N\rangle$ even in the steady-state, as long as the vibron number $\langle N_V\rangle \neq 0$. Also, the occupation of the excited states $|\phi^+_{1/2}, N\rangle$ triggers sequential tunneling-out processes to empty-molecular states $|\phi_1, N\rangle$ and $|\phi_0, N\rangle$. The intermediate charged states with $\overline{m} = 3/2$ can also be populated via tunneling-in processes.

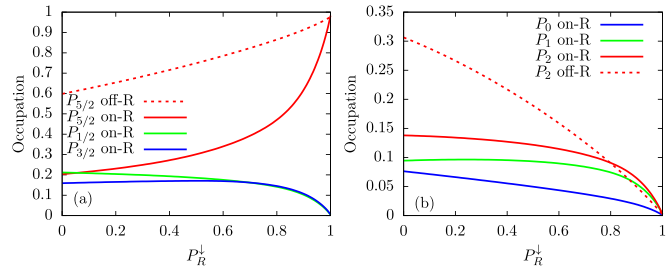

FIG. 7. Steady-state occupations as a function of $P_R^\downarrow$ in the resonant and off-resonant regime. (a) The occupations $P_{\overline{m}}$ of the charged states. (b) The occupations $P_{\overline{S}_z}$ of the empty molecular states.

To prove this scenario, we now discuss the steady-state populations of the relevant empty and charged molecular states. Figure 7 shows that in the off-resonant case the system is mostly described by states with the reverse molecular spin, namely $|\phi_{5/2}, N\rangle$ and $|\phi_2, N\rangle$, such that $P_2 + P_{5/2} > 0.9$ for all values of $P_R^\downarrow$ (the much smaller occupation of the states $|\phi^\pm_{3/2}, N\rangle$ was not shown). On the other hand, at resonance, *all* configurations with positive quantum numbers achieve substantial populations as long as $P_R^\downarrow < 0.7$. As the polarization of the right electrode increases, the occupations of states with dominant spin number $\overline{m} > 0$ and $\overline{S}_z > 0$ decrease. Eventually, for the fully antiparallel configuration $P_L^\uparrow = P_R^\downarrow = 1$ the system ends up in the polarized state, and $P_{5/2} \approx 1$ both in the resonant and off-resonant regimes.

Figure 8 adds to the analysis of the stationary properties by showing their dependence on the polarization of the right electrode. Figure 8(a) allows a comparison of the resonant and off-resonant steady-state currents. A small difference (around 6.5 pA) between the two currents is noticed even for nonmagnetic drain electrode (i.e., for $P_R^\downarrow = 0$). As $P_R^\downarrow$ increases, both currents decrease but at different slopes and eventually vanish in the fully antiparallel configuration $P_R^\downarrow = 1$, when the spin-up occupation $N_\uparrow = 1$ both in the resonant and off-resonant regimes [see Fig. 8(b)]. The mean average spin $\langle S_z\rangle$ is shown in Fig. 8(c). In the off-resonant regime, the spin reversal is rather efficient for all values of $P_R^\downarrow$ (e.g., $\langle S_z\rangle > 1.85$ even in the nonmagnetic case $P_R^\downarrow = 0$). In turn, the significant occupation of the charged and empty molecular states with $S_z \neq 2$ strongly affects the spin reversal at resonance. The mean vibron number presented in Fig. 8(d) decreases as the right electrode becomes magnetic. One notices that in the resonant regime, $\langle N_V\rangle \approx 0.2$ when $P_R^\downarrow = 1$,

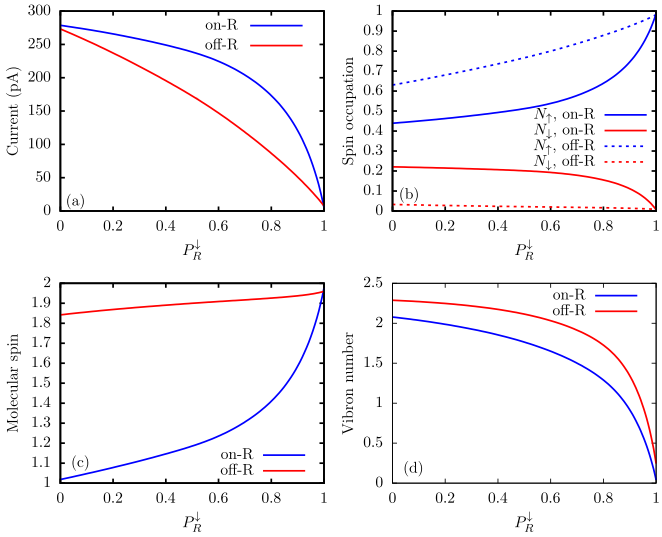

FIG. 8. Steady-state quantities as functions of $P_R^\downarrow$ in the resonant and off-resonant regimes. (a) The current J_R. (b) The spin-dependent electronic occupations N_σ. (c) The average molecular spin. (d) The mean vibron number N_V.

whereas in the off-resonant regime the vibron number almost vanishes.

In this case, we have checked that when $P_R^\downarrow = 1$, the occupation $P_{5/2}$ shown in Fig. 7(a) reduces to the occupation of the state $|\phi_{5/2}; N = 0\rangle$. On the other hand, in the resonant case we find nonvanishing populations for several excited states $|\phi_{5/2}, N > 0\rangle$. We emphasize that the behavior shown in Figs. 6(a) and 8(a) could be, in principle, reproduced in future experiments, at least for nonmagnetic or weakly polarized drain electrodes. Also, the left electrode could be a magnetized tip as in the spin-polarized scanning tunneling microscopy (SP-STM) setup.

Our analysis shows that although the polarization of the left electrode allows the spin to overcome the anisotropy barrier, the current-induced magnetic switching is damaged if the resonant regime couples the states $|\phi_{5/2}; N + 1\rangle$ and $|\phi_{1/2}^+; N\rangle$. This fact is not beneficial for efficient spin manipulation schemes, but the spin-vibron effects on the transient and stationary currents can be used to probe indirectly the resonant transitions as the molecular spin climbs down the anisotropy barrier.

In contrast, if the resonant condition favors transitions between states on different sides of the anisotropy barrier, we find that the effect of the spin-vibron coupling on the CIMS is very small. For example, if we tune the frequency of the vibrational mode to the transitions $|\phi_{-3/2}^+; N + 1\rangle \to |\phi_{1/2}^+; N\rangle$, the molecular spin switches to $\langle S_z\rangle = 2$ and we only notice small differences in the transient curves corresponding to resonant and off-resonant regimes (not shown). The negligible effect of the spin-vibron coupling in this case can be explained by the CIMS mechanism (see [24,25] and references therein): the asymmetric spin-dependent tunneling processes push the system towards the rightmost single-particle and empty states having $S_z = 2$ (i.e., $|\phi_{5/2}\rangle$ and $|\phi_2\rangle$), while the other *intermediate* spin states will eventually be depleted.

For completeness, we also discuss the case in which the hybrid system carries a nonpolarized charge current, which

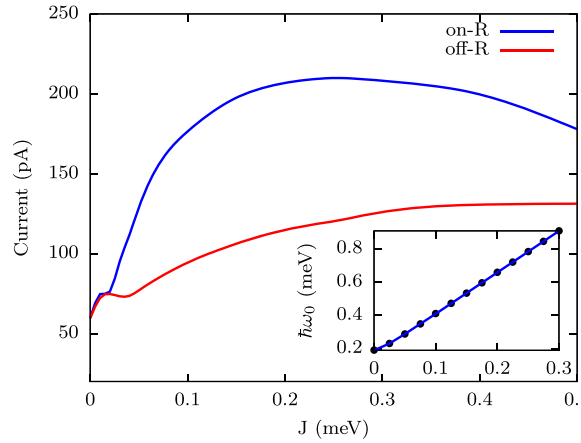

FIG. 9. Steady-state current J_S as a function of the exchange interaction strength J. Inset: the resonant energies $\hbar\omega_0$ calculated for $E = 0$ (solid line) and for $E/D = 1/15$ (filled circles). Other parameters: $P_R^\downarrow = 0.7$.

corresponds to the equal spin densities in both leads such that $P_L^\sigma = P_L^\sigma = 0$. As shown in previous papers [22,25], this configuration will not lead to a *complete* spin reversal. Performing numerical calculations for the same initial state $|\phi_{-2}; 0\rangle$, we find that the average spin increases only up to the steady-state value $\langle S_z\rangle = 0$. This feature persists even if the spin-vibron coupling activates spin transitions between the states $|\phi_{-3/2}^+; N + 1\rangle$ and $|\phi_{1/2}^+; N\rangle$. Again, slight differences between the resonant and off-resonant cases are noticed only in the transient regime (not shown).

Finally, we also inspected whether the signatures of the spin-vibron interaction on the steady-state currents can still be detected at smaller values of the exchange interaction J. Although for specific molecules J could be calculated by *ab initio* methods, in theoretical works that rely on the giant-spin effective Hamiltonian it is considered as an input parameter. In Ref. [26] the strength of the exchange interaction is denoted by $a\mu_B$, where $a = -3.9$ T; therefore, $J := |a\mu_B| \approx 0.23$ meV, in agreement with the value considered in our simulations.

In Fig. 9 we present the stationary currents J_S in the resonant and off-resonant regimes as functions of J. We stress that for each value of J, the frequency ω_0 of the vibrational mode is adjusted such that the resonant condition $E_{1/2}^+ - E_{5/2} = \hbar\omega_0$ corresponds to the same value of the magnetic field $B = 150$ mT. In fact, if the transverse anisotropy $E = 0$, the gap $E_{1/2}^+ - E_{5/2}$ can be calculated from Eq. (15). The corresponding resonant energies $\hbar\omega_0$ shown in the inset of Fig. 9 are close to the calculated values in the presence of the transverse anisotropy. One notices that as the exchange interaction decreases, the resonant transitions correspond to lower frequencies. This also means that the system enters the strong-coupling regime with respect to the electron-vibron coupling, as the ratio $\lambda/\hbar\omega_0 > 1$ for $J < 0.12$ meV.

Most importantly, Fig. 9 proves that the difference between the stationary currents in the two regimes remains significant when J covers a wide range of values. Notably, one could still detect the presence of the resonant transitions even if J is comparable to the easy-axis anisotropy coefficient

($D = 0.056$ meV). As the coupling strength decreases, the two currents drop and reach the same value for $J = 0$. This behavior can be explained by considering the effect of the exchange coupling on the spin-dependent transport. As the polarization of the left electrode is $P_L^{\uparrow} = 1$, a nonvanishing spin-down component of the current requires some exchange-induced spin-flip processes in the system. We find that as J decreases, the mixing of the spin states [see Eq. (14)] becomes negligible. Accordingly, at $J = 0$ the occupation $N_{\downarrow}$ vanishes in both regimes. Then the current is carried only by spin-up electrons and is limited by the polarization of the right electrode. At larger values of J, the stationary current slowly decreases, because at higher frequencies ω_0 the ratio $\lambda/\hbar\omega_0$ becomes smaller and affects the tunneling matrix elements [see Eqs. (24) and (6)].

We conclude our study by discussing the role of vibron relaxation. For the small values of the loss parameter κ considered in this work, the corresponding relaxation time is indeed long enough to discern the effects of the spin-vibron coupling. By further increasing the loss coefficient κ, the average number of vibrons in the stationary state will eventually decrease, and therefore the effects of the spin-vibron coupling are less visible. Nonetheless, the number of vibrons generated via tunneling processes would further increase by increasing the strength of the electron-vibron coupling or the coupling to the leads.

IV. CONCLUSIONS

In this work, we studied theoretically the interplay between the spin-vibron, charge-vibron, and exchange interactions in a single-molecule magnet coupled to spin-polarized leads. The SMM is described by an effective giant-spin Hamiltonian associated with a localized spin $S = 2$. In spite of its simplicity, this model allows us to predict specific and sizeable effects of the spin-vibron coupling on the transport properties. The transient and stationary quantities were calculated numerically from the master equation, this approach being most suitable for weak molecule-electrode coupling. To detect the vibron-assisted transitions of the molecular spin on both sides of the anisotropy barrier, we considered two quasi-antiparallel configurations of the electrodes, namely $\downarrow_L\uparrow_R$ and $\uparrow_L\downarrow_R$. All results are conveniently explained using the vibron-dressed states picture and the Jaynes-Cummings model from quantum optics.

We find that the antiparallel configuration $\downarrow_L\uparrow_R$ induces a spin-blockade in the off-resonant regime. In contrast, the resonant regime allows the indirect reading of the spin transitions on the left side of the anisotropy barrier. The numerical results predict an enhancement of the steady-state current in the resonant regime and periodic or quasiperiodic Rabi oscillations of the transient current. More precisely, the stationary current develops a peak as the magnetic field applied on the easy-axis of the SMM sweeps the resonance. The observation of such peaks in future experiments would confirm the existence of transitions induced by the spin-vibron coupling, and it provides a useful investigation tool, given the fact that the vibrational modes or the strengths of the exchange and spin-vibron interactions for specific molecules are not easy to compute.

In the second configuration, $\uparrow_L\downarrow_R$, the spin-vibron coupling induces transitions on the right side of the anisotropy barrier which compete with the magnetic switching due to tunneling processes. Although in this case the Rabi oscillations in the transient regime cannot be discerned anymore, we find that the resonant transitions still induce an important amplification of the stationary currents for a wide range of the polarization parameters of the drain electrode.

Let us stress that in previous experiments [14,15], the effects of the spin-vibron coupling were identified by reversing the molecular spin via the mechanism of quantum tunneling of magnetization in an *indirect* transport setting, i.e., when the molecule is not connected to electrodes but rigidly attached to a conducting nanoresonator. Our results provide insight into a new facet of the spin-vibron interaction and predict that its effects could also be observed in the *direct* transport configuration. In this setup, the vibron-assisted spin transitions and the exchange interaction between the localized spin and electrons tunneling through the molecular orbitals cannot be disentangled. Each of these two interactions plays an important role in transport. The exchange interaction allows the climbing of the anisotropy barrier via the current-induced magnetic switching, whereas the spin-vibron coupling brings in additional transitions of the molecular spin. On the other hand, the resonant transitions and therefore the spin-vibron coupling can be conveniently switched-on and -off by varying the magnetic field.

ACKNOWLEDGMENTS

This work is funded by the Core Program of the National Institute of Materials Physics, granted by the Romanian Ministry of Research, Innovation and Digitalization under Project No. PC2-PN23080202.

[1] D. Gatteschi, R. Sessoli, and J. Villain, *Molecular Nanomagnets* (Oxford University Press, Oxford, 2006).

[2] *Molecular Magnets*, edited by J. Bartolomé, F. Luis, and J. F. Fernández, NanoScience and Technology (Springer, Berlin, Heidelberg, 2014).

[3] E. Burzurí, R. Gaudenzi, and H. S. J. van der Zant, J. Phys.: Condens. Matter **27**, 113202 (2015).

[4] M. Slota and L. Bogani, Appl. Magn. Reson. **51**, 1357 (2020).

[5] E. Moreno-Pineda and W. Wernsdorfer, Nat. Rev. Phys. **3**, 645 (2021).

[6] A. Gaita-Arinñ, F. Luis, S. Hill, and E. Coronado, Nat. Chem. **11**, 301 (2019).

[7] C. Godfrin, A. Ferhat, R. Ballou, S. Klyatskaya, M. Ruben, W. Wernsdorfer, and F. Balestro, Phys. Rev. Lett. **119**, 187702 (2017).

[8] M. D. Jenkins, Y. Duan, B. Diosdado, J. J. García-Ripoll, A. Gaita-Ariño, C. Giménez-Saiz, P. J. Alonso, E. Coronado, and F. Luis, Phys. Rev. B **95**, 064423 (2017).

[9] A. Castro, A. García Carrizo, S. Roca, D. Zueco, and F. Luis, Phys. Rev. Appl. **17**, 064028 (2022).

[10] A. S. Zyazin, J. W. G. van den Berg, E. A. Osorio, H. S. J. van der Zant, N. P. Konstantinidis, M. Leijnse, M. R. Wegewijs, F. May, W. Hofstetter, C. Danieli, and A. Cornia, Nano Lett. **10**, 3307 (2010).
[11] M. Misiorny, E. Burzurí, R. Gaudenzi, K. Park, M. Leijnse, M. R. Wegewijs, J. Paaske, A. Cornia, and H. S. J. van der Zant, Phys. Rev. B **91**, 035442 (2015).
[12] J. Koch, F. von Oppen, and A. V. Andreev, Phys. Rev. B **74**, 205438 (2006).
[13] E. Burzurí, Y. Yamamoto, M. Warnock, X. Zhong, K. Park, A. Cornia, and H. S. J. van der Zant, Nano Lett. **14**, 3191 (2014).
[14] M. Ganzhorn, S. Klyatskaya, M. Ruben, and W. Wernsdorfer, Nat. Nanotechnol. **8**, 165 (2013).
[15] M. Ganzhorn, S. Klyatskaya, M. Ruben, and W. Wernsdorfer, Nat. Commun. **7**, 11443 (2016).
[16] J. F. Nossa, M. F. Islam, C. M. Canali, and M. R. Pederson, Phys. Rev. B **88**, 224423 (2013).
[17] N. Gallego-Planas, A. Martín-Rodríguez, and E. Ruiz, Dalton Trans. **45**, 18867 (2016).
[18] A. McCaskey, Y. Yamamoto, M. Warnock, E. Burzurí, H. S. J. van der Zant, and K. Park, Phys. Rev. B **91**, 125419 (2015).
[19] A. Chiesa, E. Macaluso, P. Santini, S. Carretta, and E. Pavarini, Phys. Rev. B **99**, 235145 (2019).
[20] A. Mattioni, J. K. Staab, W. J. A. Blackmore, D. Reta, J. Iles-Smith, A. Nazir, and N. F. Chilton, arXiv:2301.05557.
[21] C. Timm and F. Elste, Phys. Rev. B **73**, 235304 (2006).
[22] M. Misiorny and J. Barnaś, Phys. Rev. B **76**, 054448 (2007).
[23] M. Misiorny and J. Barnaś, Phys. Rev. Lett. **111**, 046603 (2013).
[24] V. Moldoveanu, I. V. Dinu, B. Tanatar, and C. P. Moca, New J. Phys. **17**, 083020 (2015).
[25] M. Misiorny and J. Barnaś, Phys. Status Solidi B **246**, 695 (2009).
[26] C. Godfrin, S. Thiele, A. Ferhat, S. Klyatskaya, M. Ruben, W. Wernsdorfer, and F. Balestro, ACS Nano **11**, 3984 (2017).
[27] F. May, M. R. Wegewijs, and W. Hofstetter, Beilst. J. Nanotechnol. **2**, 693 (2011).
[28] J. Brüggemann, S. Weiss, P. Nalbach, and M. Thorwart, Phys. Rev. Lett. **113**, 076602 (2014).
[29] J. Brüggemann, S. Weiss, P. Nalbach, and M. Thorwart, New J. Phys. **18**, 023026 (2016).
[30] A. Kenawy, J. Splettstoesser, and M. Misiorny, Phys. Rev. B **97**, 235441 (2018).
[31] L. Cai, R. Jaafar, and E. M. Chudnovsky, Phys. Rev. Appl. **1**, 054001 (2014).
[32] V. Moldoveanu and R. Dragomir, Phys. Rev. B **104**, 075441 (2021).
[33] K. Hymas and A. Soncini, Phys. Rev. B **99**, 245404 (2019).
[34] K. Hymas and A. Soncini, Phys. Rev. B **102**, 045313 (2020).
[35] E. M. Chudnovsky, D. A. Garanin, and R. Schilling, Phys. Rev. B **72**, 094426 (2005).
[36] C. Caroli, R. Combescot, P. Nozieres, and D. Saint-James, J. Phys. C **4**, 916 (1971).
[37] V. Moldoveanu, A. Manolescu, and V. Gudmundsson, Entropy **21**, 731 (2019).
[38] D. W. Utami, H.-S. Goan, and G. J. Milburn, Phys. Rev. B **70**, 075303 (2004).
[39] J. S. Ferreira and P. Ribeiro, Phys. Rev. B **100**, 184422 (2019).
[40] H. J. Lipkin, N. Meshkov, and A. J. Glick, Nucl. Phys. **62**, 188 (1965).
[41] M. Kaczor, I. Tralle, P. Jakubczyk, S. Stagraczyński, and L. Chotorlishvili, Ann. Phys. **442**, 168918 (2022).
[42] The calculated frequencies of the vibrational modes of a Fe_4 SMM are larger than this value, but of the same order of magnitude (the frequencies reported in Ref. [18] correspond to energies $\hbar\omega_0$ in the range 1.9–3.4 meV). For the system considered here, transitions between the states $|\phi_{-5/2}; N+1\rangle$ and $|\phi^{-}_{-1/2}; N\rangle$ require a smaller frequency, $\hbar\omega_0 = 0.24$ meV.
[43] M. O. Scully and M. S. Zubairy, *Quantum Optics* (Cambridge University Press, Cambridge, 1997).
[44] Note that in Fig. 3(a) we represented only energies that are very sensitive to the spin-vibron coupling. The whole spectrum is more complex, and most of its energies depend linearly on the magnetic field through the Zeeman shifts. The resemblance of the partial spectrum shown in Fig. 3(a) to the Jaynes-Cummings spectrum does not mean that the SMM system can be described by an effective two-level model.